AGU PUBLICATIONS

Water Resources Research

TECHNICAL REPORTS: METHODS

10.1002/2015WR018441

Merging radar and in situ rainfall measurements: An assessment of different combination algorithms

Mohammad Mahadi Hasan[1], Ashish Sharma[1], Fiona Johnson[1], Gregoire Mariethoz[1,2], and Alan Seed[1,3]

[1]School of Civil and Environmental Engineering, University of New South Wales, Sydney, New South Wales, Australia, [2]Institute of Earth Surface Dynamics, University of Lausanne, Lausanne, Switzerland, [3]Research and Development, Bureau of Meteorology, Australia

Abstract Merging radar and gauge rainfall estimates is an area of active research. Since rain gauges alone are often limited at representing the complete spatial distribution of rainfall, a combination of radar-derived rainfall with spatially interpolated gauge estimates using alternate weighting approaches is investigated. This paper examines several merging methods that differ in the consideration of correlation among the estimation errors, their distribution, and the application of dynamic and static weighting. The merging process has been applied to the radar data from Terrey Hills radar located in Sydney, Australia, and spatially interpolated gauge rainfall on the same area. The performance of the merging methods is assessed by comparing the combined estimate with the gauge observation. It is however clear from our findings that rainfall estimation from any of the combination approaches assessed contains less error than any of the noncombination approaches. The results show that the correlation between these two rainfall estimation errors plays a significant role in the performance of the merging methods. The combination method should be chosen depending on the purpose, accuracy of the estimate, and complexity of the method.

Key Points:
- The influence of error independence (uncorrelated and correlated) on the combined estimates
- The effect of static or dynamic weighting on the combined estimates
- The consequence of Gaussian or non-Gaussian error distributions on the combined estimates

Correspondence to:
A. Sharma,
a.sharma@unsw.edu.au

Citation:
Hasan, M. M., A. Sharma, F. Johnson, G. Mariethoz, and A. Seed (2016), Merging radar and in situ rainfall measurements: An assessment of different combination algorithms, *Water Resour. Res.*, *52*, doi:10.1002/2015WR018441.

Received 30 NOV 2015
Accepted 21 SEP 2016
Accepted article online 27 SEP 2016

1. Introduction

Rainfall estimates at a high temporal and spatial resolution are vital for hydrological sciences and their applications [*Delrieu et al*., 2014; *Sideris et al*., 2014]. The two most commonly used means for rainfall measurement are the ground-based rain gauge networks traditionally used, and the remotely sensed measurements obtained using weather radars [*Krajewski and Smith*, 2002; *Velasco-Forero et al*., 2009; *Woldemeskel et al*., 2013]. Though radar and gauge rainfall estimates are fairly correlated [*Creutin et al*., 1988], gauges provide accurate rainfall estimates at point locations whereas radar provides rainfall estimates over a widespread domain [*Berndt et al*., 2014; *Hasan et al*., 2014]. However, concerns about the biases in radar rainfall estimates hampers their direct use in hydrological studies [*Mandapaka et al*., 2009; *Mandapaka et al*., 2010; *Seo and Breidenbach*, 2002; *Smith et al*., 2007; *Villarini et al*., 2008; *Zhang and Smith*, 2003]. On the other hand, the spatial representativeness of gauge rainfall can be poor as gauges are often sparsely distributed over a catchment, particularly in areas of high relief where there may be large rainfall gradients. Given these potential weaknesses in both data sources, what can be done to provide better rainfall estimates?

The idea of merging radar and gauge measurement has become popular for estimating ground rainfall by exploiting the strength and minimizing the weaknesses of each method [*Goudenhoofdt and Delobbe*, 2009; *Haberlandt*, 2007]. The concept of combining different estimates of the same event has gained wide acceptance. The rationale behind the combination of multiple sources is that the individual model/method contains errors from various sources. Each source of error affects each estimation method in a particular way. The combination of several model estimates therefore allows minimizing these errors, resulting in better predictions compared to the single best model [*Ajami et al*., 2006; *Stock and Watson*, 2004].

The idea of combining multiple outputs is widely used in the field of econometrics [*Bates and Granger*, 1969; *Genre et al*., 2013; *Hall and Mitchell*, 2007; *Timmermann*, 2006]. Model combination approaches have been applied in hydrology and climate science, including streamflow simulation and forecasting [*Ajami et al*., 2006; *Georgakakos et al*., 2004], rainfall-runoff modeling [*Shamseldin and O'Connor*, 1999] as well as

weather and climate models [*Chowdhury and Sharma*, 2009; *Khan et al*., 2014; *Krishnamurti et al*., 1999; *Krishnamurti et al*., 2000].

A number of different methods have been developed to merge radar and gauge rainfall estimates such as Mean Field Bias [*Berndt et al*., 2014; *Borga et al*., 2002; *Seo and Breidenbach*, 2002; *Smith and Krajewski*, 1991], Kalman Filter [*Chumchean et al*., 2006a], and geostatistical approaches. The geostatistical approaches include Kriging, Cokriging, and Kriging with external drift [*Berndt et al*., 2014; *Goudenhoofdt and Delobbe*, 2009; *Haberlandt*, 2007; *Sideris et al*., 2014; *Velasco-Forero et al*., 2009]. This geostatistical merging is done by applying two different approaches [*Jewell and Gaussiat*, 2015]. In the first approach, initially the gauge rainfall is spatially interpolated independently of the radar, and then the difference between radar and spatially interpolated gauge rainfall is added to the radar rainfall to get an estimate at an unknown location. This idea is used in kriging with radar-based error correction [*Ehret et al*., 2008] and conditional merging [*Sinclair and Pegram*, 2005]. In the second approach, before the generation of the interpolated field, the radar estimate at ungauged locations is formulated using weights. The weights are determined from the relationship between the measured radar and gauge rainfall at gauged locations. All those studies consider the radar data as secondary information, which are used to improve the spatially interpolated gauge rainfall [*Goudenhoofdt and Delobbe*, 2009]. There are also differences in combination approaches whether the weights vary in time (dynamic weighting) [*Chowdhury and Sharma*, 2010; *Krishnamurti et al*., 1999] or not (static weighting) [*Allard et al*., 2012; *Robertson et al*., 2004; *Timmermann*, 2006]. *Hasan et al*. [2016] used a weighted combination approach to merge radar and spatially interpolated gauge rainfall estimates, assuming that the errors from the multiple estimates are correlated. This study investigates the effect of different merging techniques such as static and dynamic weighing as well as point [*Chowdhury and Sharma*, 2009; *Genre et al*., 2013; *Smith and Wallis*, 2009; *Timmermann*, 2006] and density-based merging [*Allard et al*., 2012; *Clemen and Winkler*, 2007; *Liu et al*., 2012; *Ranjan*, 2009], given that mean and variance of radar and gauge estimates are known. This study does not give priority to gauge measurements over radar rainfall estimates, rather considers that both radar and gauge provide useful information. The importance of each is given based on the estimation error. While kriging-based approaches are not explicitly included in our comparison, in principle they have similarities to the Copula-based approach [*Bárdossy*, 2006; *Bárdossy and Li*, 2008; *Durante and Sempi*, 2010] which is included.

The previous studies on radar and gauge combination approaches did not consider the implication of error independence, error distributions and static versus dynamic weighting on the merged estimates. The focus of this study is to investigate the merits and demerits of alternative combination approach in the context of radar rainfall estimation. It is expected that the outcomes reported here can be used as a guide when choosing the optimal merging algorithm in a wide range of practical settings.

The rest of this paper is organized as follows. The different merging approaches are presented in section 2. Section 3 presents the data used in this study. The performance of the different merging approaches is discussed in section 4. Finally, discussion and conclusion are presented in section 5.

2. Merging Methods

Model merging is based on the idea that the weighted average of multiple methods can provide a better quantity of interest than any single method. This is particularly the case when the errors from the different methods are complementary, in the sense that one method tends to perform well where other methods are weak. A literature review of combination methods suggests that there are a number of approaches available to determine these weights. In this paper, we consider six different methods that have been found to be useful in previous studies. As discussed above, there are three main distinctions that can be made between the methods:

1. Correlated or uncorrelated errors from the multiple methods
2. Static or dynamic weighting
3. Gaussian or non-Gaussian error distributions around the estimates

According to these three criteria, the six methods are summarized in Table 1 along with details of their previous applications.

Table 1. Different Merging Approaches

	Name	Error Correlation Structure	Weighting Type	Error Distribution	Reference
1	Error variance method	Uncorrelated errors	Dynamic	Gaussian	*Bates and Granger* [1969], *Smith and Wallis* [2009], and *Wasko et al.* [2013]
2	Error covariance method	Correlated errors	Dynamic	Gaussian	*Khan et al.* [2014] and *Timmermann* [2006]
3	Error rotation method	Decorrelated errors	Dynamic	Gaussian	*Fortuna and Capson* [2004], *Khan et al.* [2014], and *Shih-Hau et al.* [2008]
4	PDF overlap method	Uncorrelated errors	Dynamic	Gaussian and non-Gaussian	*Liu et al.* [2012]
5	Probability aggregation method	Conditional independence errors	Static	Gaussian	*Allard et al.* [2012], *Clemen* [1989], *Clemen and Winkler* [2007], *Gneiting and Ranjan* [2013], and *Ranjan* [2009]

The following example illustrates the workings of these merging methods. Let R_A and R_B be the estimates from two different methods A and B, e_A and e_B are the estimation errors, and ρ is the correlation between estimation errors. The estimation errors are the differences between observations (R_O) and corresponding estimates (i.e., $e_A = R_O - R_A$ and $e_B = R_O - R_B$). $\sigma^2{}_A$ and $\sigma^2{}_B$ are the variance of the estimation errors. W_A and W_B are the weights in the combined estimate. The basic equation for combination, assuming two methods, A and B is

$$R_{COM,\ t} = W_{A,t}R_{A,t} + W_{B,t}R_{B,t} \tag{1}$$

where for time step t, $R_{A,t}$ and $R_{B,t}$ are the estimates obtained from the two different methods A and B. $W_{A,t}$ and $W_{B,t}$ are the weights applied to each method to provide a combined estimate $R_{COM,t}$. The question is to determine the time-varying weights $W_{A,t}$ and $W_{B,t}$.

The following section will describe each of these methods, their advantages and drawbacks and the procedure for estimating the weights. To make a fair comparison, we have used a common data set to compare all methods, and have divided the data set into calibration and validation periods. The required weights are calculated using the calibration data set. Finally, the performance of different methods is compared using the results obtained from the validation data set.

2.1. Error Variance Method

In this approach, the estimates are combined according to weights that are calculated from variances of estimation errors [*Smith and Wallis*, 2009]. In the combined estimate, the method with better estimates is given greater weight. One of the major assumptions of this approach is that the errors from the multiple methods are uncorrelated. It is also assumed that the errors of individual estimates are normally distributed and unbiased. The combined estimates are unbiased because the sum of the weights equals to one [*Timmermann*, 2006].

The weights of method A and B can be estimated by equations (2) and (3), given below:

$$W_A = \frac{\sigma_B^2}{\sigma_A^2 + \sigma_B^2} \tag{2}$$

$$W_B = \frac{\sigma_A^2}{\sigma_A^2 + \sigma_B^2} \tag{3}$$

2.2. Error Covariance Method

The previous method assumed uncorrelated errors, while it is clearly not the case in many circumstances. Therefore, it is possible to extend the method by including the correlation between estimation errors. The estimates from different methods are combined using the weighted average of estimates. The weight is calculated using a variance and covariance of estimates [*Timmermann*, 2006]. Minimizing the quantity in equation (4), given below, can estimate weights of methods A and B as:

$$\min\ \left(W' \sum\nolimits_e W\right)\ \text{such that}\ W'I = 1 \tag{4}$$

where, $W' = [W_A \quad W_B]$, $\sum_e$ is the covariance matrix of the estimation errors, off-diagonals are the covariance of the errors and diagonals are the variance of the errors from the two methods. I is a m by 1 column

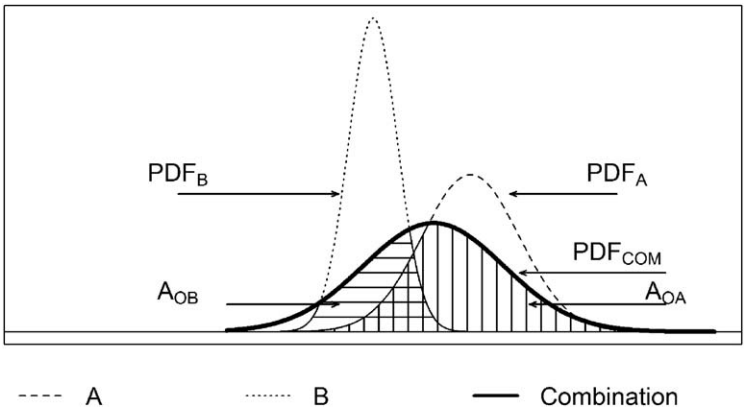

Figure 1. Illustration of the PDF overlap (Gaussian) approach. PDF_A and PDF_B represent the PDF of the two estimates by methods A and B. PDF_{COM} is the PDF of the combined estimate. A_{OA} and A_{OB} denote the overlapping area contributed by methods A and B.

vector of ones with *m* denoting the number of methods. Here we have two methods (A and B), so $m = 2$. The weights constrained to add up to unity and lie between 0 and 1. Readers are referred to *Timmermann* [2006] for further details concerning the derivation of equation (4).

2.3. Error Rotation Method

One way to process correlated errors is to transform them to decorrelated values [*Fortuna and Capson*, 2004; *Qian and Fowler*, 2007; *Shih-Hau et al*., 2008]. This method is similar to the error covariance method, except that the correlation between errors is forced to zero. The decorrelation is done by applying principal component analysis (PCA) [*Genre et al*., 2013; *Stock and Watson*, 2002, 2004]. In the rotated space, the decorrelated estimation errors are used to estimate the combination weights. Finally, those weights are rotated back onto the original space.

The procedure adopted is as follows:

1. Compute uncorrelated errors ($\acute{e}_A$, $\acute{e}_B$) by applying PCA to the estimation errors (e_A, e_B).
2. Calculate the weights ($\acute{W}_A$, $\acute{W}_B$) in the transformed space using equation (4).
3. Back-transform the calculated weights ($\acute{W}_A$, $\acute{W}_B$) into the original space by applying the inverse rotation and rescale them so that the weights add to one.

2.4. PDF Overlap Method

The idea behind this approach is to determine an empirical probability density function (PDF) that has the maximum overlap with the PDFs of the estimates of each individual method used [*Liu et al*., 2012]. It is an iterative process where the area of the combined PDF is determined through by a numerical optimization that maximizes the area of the combined PDF. The proportion of the area contributing the combined PDF determines the weights. This idea is illustrated in Figure 1 where the two separate estimates are assumed to have Gaussian distributions.

Although Figure 1 illustrates the idea using two assumed Gaussian distributions, the method is general such that any distribution can be used. In this study, we have investigated both the Gaussian and non-Gaussian cases. Suppose, PDF_A and PDF_B represent the PDF of the two estimates by methods A and B. PDF_{COM} is the PDF of the combined estimate. The weight for method A (W_A) is estimated by the overlapping area between PDF_{COM} and PDF_A. The overlapping area between the PDF_{COM} and PDF_B gives the weight of method B (W_B). The summation of W_A and W_B equals one.

The procedure adopted is as follows:

1. Assume initial weights for methods A and B such that they add up to one. We have initialized the weight iteration by setting $W_A = W_B = 0.50$.
2. Calculate the cumulative distribution functions (CDF) as F_A, F_B from the respective PDF_A and PDF_B.
3. Find the combined CDF from the two individual estimates

$$F_{COM} = W_A F_A + W_B F_B \tag{5}$$

4. Estimate the overlapping area contributed by methods A and B as:

$$A_{OA} = \sum_{j=1}^{n} \min\left[p^j_{COM} \quad p^j_A \right] \tag{6}$$

$$A_{OB} = \sum_{j=1}^{n} \min\left[p^j_{COM} \quad p^j_B \right] \tag{7}$$

where, A_{OA} and A_{OB} are the overlapping area contributed by the PDF_A and PDF_B, respectively. p^j_{COM}, p^j_A, and p^j_B are the probability related to the Combination, A, and B, respectively, at any section j (j = 1, 2. . ..n). p^j_{COM}, p^j_A, and p^j_B can be estimated by subtracting the probability of two consecutive sections from their respective CDF.

5. Estimate the total overlapping area A_{COM} as:

$$A_{COM} = A_{OA} + A_{OB} \tag{8}$$

6. Estimate the weight of PDF_A and PDF_B from the overlapping area as:

$$W_A = \frac{A_{OA}}{A_{OA} + A_{OB}} \tag{9}$$

$$W_B = \frac{A_{OB}}{A_{OA} + A_{OB}} \tag{10}$$

7. Then follow the steps provided in 3–5 using the weight calculated in step 5. Each iteration offers a new sets of weights along with the total overlapping area. Finally, the stopping criterion of the weight maximization approach is given by a prespecified tolerance (δ) [*Liu et al*., 2012] defined as the summation of the difference in weights produced in two consecutive iterations of the methods A and B.

$$\delta = |W_A^{j-1} - W_A^j| + |W_B^{j-1} - W_B^j| \tag{11}$$

The PDF overlap method is sufficiently general to be implemented with any distribution. Section 3 explains the practical example of Gaussian and non-Gaussian PDF overlap methods.

2.5. Probability Aggregation Method

The probability aggregation method merges two different sources of information in a probabilistic framework. Previous studies of probability relationship between two variables suggest that it can be applied to combine any distribution that represents the same physical quantity [*Allard et al*., 2012; *Marietho z et al*., 2009; *Tarantola*, 2005]. There are many ways of probability aggregation reported in [*Allard et al*., 2012] such as additive method (linear pooling, beta-transformed linear pooling), multiplication of probabilities (log linear pooling, generalized logarithmic pooling, maximum entropy approach), multiplication of odds (Tau-model, Nu-model), etc. The linear pool is a method of combining individual probability forecasts linearly according to their weights. *Ranjan and Gneiting* [2010] reported that linear pool is suboptimal. Methods based on the product of probabilities are superior to all other methods [*Allard et al*., 2012]. Therefore, in this paper, we have applied the product of probabilities (log linear pooling) method. The following example illustrates this probability aggregation method.

Let PDF_A and PDF_B represent the PDFs of estimates by methods A and B. $PDF_A(x;R_A)$ is the PDF ordinate for method A at location x derived as a Normal distribution centered at the estimated mean R_A. Similarly, $PDF_B(x;R_B)$ is the PDF for method B at the same location x using a Normal distribution with mean R_B that can be derived using an exogenous variable, in this case the radar reflectivity Z as explained later. Using the concept of probability aggregation, these two distributions are combined into a single one using the following equation:

$$PDF_{COM}(x) = \frac{[PDF_A(x;R_A)]^{W_A}[PDF_B(x;R_B)]^{W_B}}{\int [PDF_A(x;R_A)]^{W_A}[PDF_B(x;R_B)]^{W_B} dx} \tag{12}$$

where $PDF_{COM}(x)$ is the PDF of the combined estimate, and the denominator is a normalizing factor that ensures the resulting PDF integrates to unity.

It is important to note that the weight estimation in this method differs from that in the other methods. The weight remains constant over all the events and the approach is termed a static method. The required weights are calculated using the calibration data set. More details on obtaining this static weight are presented in the next section.

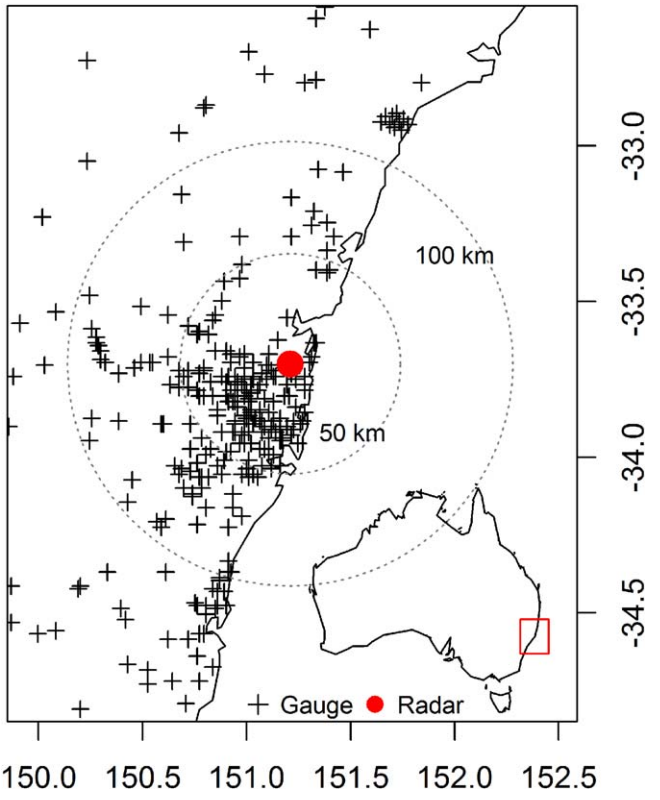

Figure 2. Study region around the Sydney Terrey Hills radar showing the gauge locations and radar location.

3. Data and Application

This section presents the results from an evaluation of the six radar and rain gauge merging approaches over the Sydney region. Radar data are obtained from the Sydney Terrey Hills radar. This radar is an S-band Doppler radar with a bandwidth of 1° and wavelength of 10.7 cm. It covers a 256 km by 256 km region with 1 km spatial resolution and 6 min temporal resolution. We have selected 1992 half hour rainfall events by visual inspection from the period from November 2009 to December 2011. In order to avoid noise and hail effects, radar reflectivities were limited between 15 and 53 dBZ [*Chumchean et al*., 2004, 2006a].

There are 282 gauges located within the study region with data during the analysis period (Figure 2). The gauges have a bucket size of either 0.2 mm or 0.5 mm size. A minimum threshold value of 1 mm/h is adopted for gauge rainfall to avoid errors from low-intensity events [*Chumchean et al*., 2004; *Chumchean et al*., 2006b]. Three different validation approaches, namely temporal, spatial, and spatio-temporal are used to assess performance of merged estimates. In the temporal validation, the available data divided into two periods one for calibration (1035 half hour rainfall events) and another one for validation (957 rainfall events). In the spatial validation [*Goudenhoofdt and Delobbe*, 2009], the available gauges are spatially divided into a calibration set (n = 158) and a validation set (n = 124) as shown in Figure 3. In the spatiotemporal validation, the two sets of gauges are used with different time period for calibration and validation. The rainfall event selection is subjective and randomly selected for calibration and validation.

Radar rainfall at the radar pixel location are estimated using a nonparametric radar rainfall estimation method (NPR method) [*Hasan et al*., 2016]. The NPR method provides better radar rainfall estimates compared to the parametric Z-R relationship [*Hasan et al*., 2016]. The kernel-based NPR method models the joint pdf between reflectivity and rainfall using kernel smoothing [*Silverman*, 1986]. Each pair of radar reflectivity and rainfall values corresponds to the mean of a Gaussian kernel. The standard deviation (or bandwidth) of kernels is given by the conditional covariance. For each kernel, conditional weight and conditional mean are estimated. The expected radar rainfall can be obtained from the locally weighted average of all kernels. We have interpolated the gauge observations using the copula-based spatial interpolation (CSI) technique described in *Wasko et al.* [2013]. The gauge observations at any radar pixel location is interpolated excluding coincident gauge observations at the pixel and using only the remaining observations. The interpolated rainfall is the weighted contribution of the nearest neighbor gauges with weights depending on the covariance of the nearest measurements and the distance between radar pixel and gauge locations [*Delrieu et al*., 2014; *Jewell and Gaussiat*, 2015; *Velasco-Forero et al*., 2009]. We have used the leave-one-out cross-validation technique [*Goovaerts*, 2000] to implement the CSI method developed by *Wasko et al.* [2013] and *Kazianka* [2013]. Future research can be carried out by replacing the CSI estimates with any other interpolation technique such as kriging, as long as they provide mean and variance.

In the following section, methods A and B will be substituted by the CSI and NPR methods, respectively. Then, rainfall estimates (R_A and R_B), variance of estimation errors (σ^2_A and σ^2_B), and weights in the combined

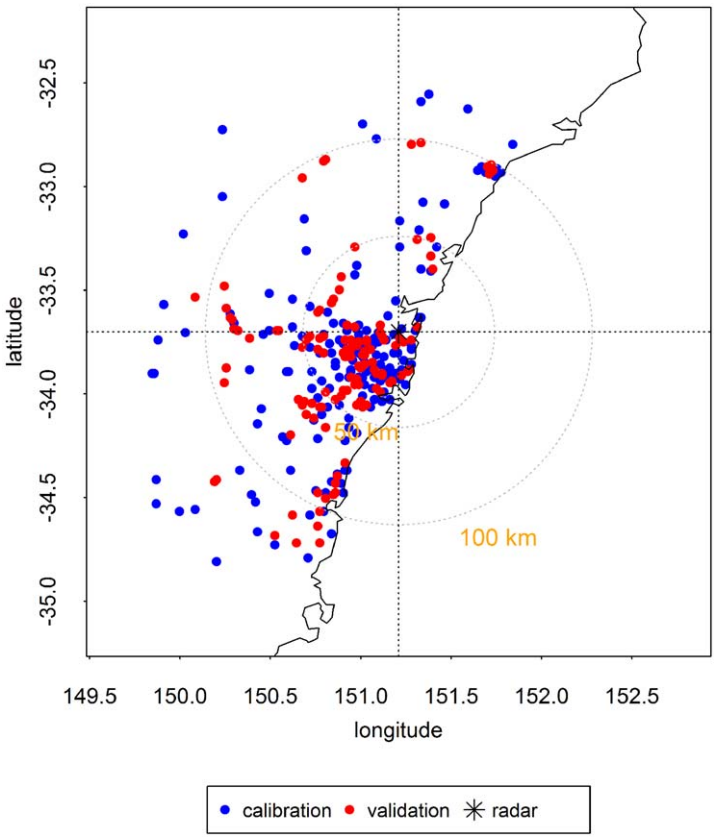

Figure 3. Spatial validation. Red color represents validation gauges and blue color represents calibration gauges.

estimate (W_A and W_B) represent the CSI and NPR methods, respectively. The weights in error variance method are obtained using equations (2) and (3). Similarly, weights in error covariance method are estimated using equation (4). The error covariance matrix in equation (4) is obtained from CSI and NPR estimation errors [*Hasan et al.*, 2016]. The error rotation method combines decorrelated CSI and NPR estimates. The PDF overlap and probability aggregation methods require a PDF estimate of the rainfall. The CSI and NPR PDFs are formulated from the mean and variance of the respective estimates (CSI and NPR) with the assumption of a Normal distribution. The Gaussian PDF merging is performed using the two normal distribution PDFs (PDF_{CSI} and PDF_{NPR}). We have also tested the non-Gaussian PDF overlap. The non-Gaussian PDF overlap is similar to the Gaussian PDF overlap method except that the non-Gaussian NPR PDF is used in the combination instead of a Gaussian NPR PDF. The non-Gaussian NPR PDF is derived from the conditional distribution of the NPR estimate (equation (13)). Given radar reflectivity (Z), the conditional probability density of rainfall (R_{NPR}) can be estimated as (see *Hasan et al.* [2016] and *Sharma et al.* [1997] for details):

$$\hat{f}(R_{NPR}|Z)=\frac{1}{n}\sum_{i=1}^{n}\frac{1}{(2\pi\lambda^2 S_c)^{1/2}}w_i\exp\left(-\frac{(R_{NPR}-b_i)^2}{2\lambda^2 S_c}\right) \tag{13}$$

where w_i is the conditional weight and b_i is the conditional mean associated with the ith kernel, λ is the bandwidth, and S_c is the conditional covariance of rainfall-reflectivity pairs that measure the spread of the conditional probability density.

In most of the cases, the non-Gaussian NPR PDF provides longer tail distributions which have advantages in the estimation of extremes. As the use of a Gaussian PDF may result in probability density for negative values of rainfall, we have incorporated the widely used reflection technique [*Jones*, 1993; *Karunamuni and Alberts*, 2005a; *Karunamuni and Alberts*, 2005b; *Silverman*, 1986] at the boundary to avoid any negative expected values. However, this issue was not faced with the sample data used in our study, as no negative estimates were noted.

The probability aggregation method requires prespecification of CSI and NPR weights (W_A, W_B) in the combination process. We have calibrated the weight by using 64 possible pairs of W_A, W_B on a calibration data set. The weights are allowed to vary from 0 to 3.5 with a step of 0.50. The RMSE of each pair is computed by comparing to the observation. The pair that gives minimum RMSE is used for validation. The results of the sensitivity analysis are shown in Figure 4. The CSI and NPR weights are shown in two axes. Depending on the W_A and W_B pairs RMSE varies from 2.7 to 4.5 mm/h. In general, RMSE increases when the weight (W_A, W_B) increase.

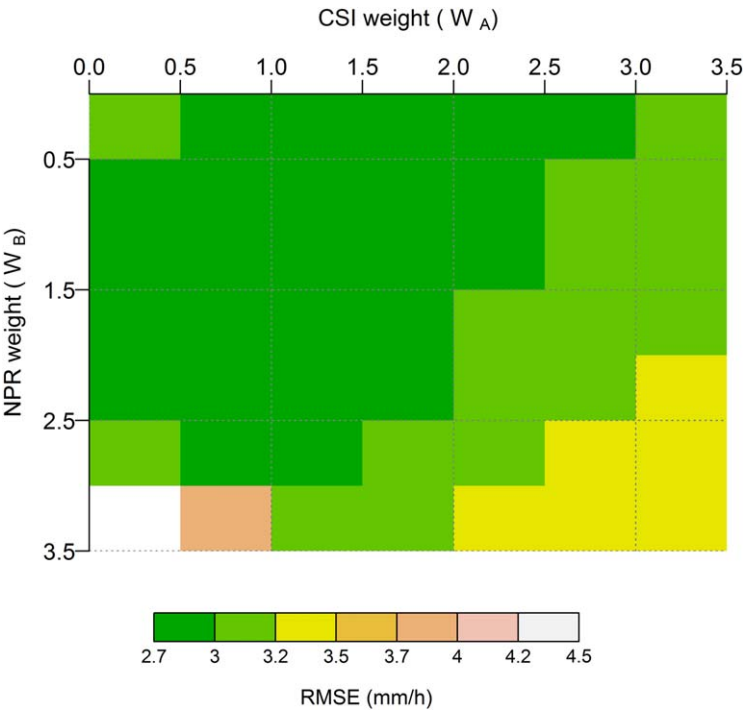

Figure 4. Sensitivity analysis of CSI and NPR weights used in the probability aggregation method.

4. Results

The radar and gauge rainfall are calculated at each radar pixel using the NPR and CSI methods for each half hour rainfall event. Then these two estimates are combined using the six different combination approaches described in section 2. The performance of these combination methods is evaluated using the root-mean-square error (RMSE), mean absolute error (MAE), percent bias (PBIAS), and median absolute error (Median AE) by comparing with the gauge observations. These measures are calculated as follows:

$$\mathrm{RMSE}=\sqrt{\frac{1}{n}\sum_{i=1}^{n}(R_{est}-R_g)^2} \quad (14)$$

$$\mathrm{MAE}=\frac{1}{n}\sum_{i=1}^{n}|R_{est}-R_g| \quad (15)$$

$$\mathrm{PBIAS}=100*\frac{1}{n}\sum_{i=1}^{n}\left(\frac{R_{est}-R_g}{R_g}\right) \quad (16)$$

$$\mathrm{logerror}=10\ \log_{10}\left(\frac{R_{est}}{R_g}\right) \quad (17)$$

$$\mathrm{AE}=|R_{est}-R_g| \quad (18)$$

where R_g represents gauge rainfall and R_{est} represents the rainfall estimated using one of the six methods. A summary of the results for the different combination approaches is given in Table 2 based on the validation period.

The results displayed in Table 2 show that the PDF overlap (non-Gaussian) method is superior to the rest of the approaches in terms of RMSE. The probability aggregation method gives the best result in terms of MAE, PBIAS, and Median AE among the methods. It is important to note that RMSE gives a relatively high

Table 2. Temporal (T), Spatial (S), and Spatiotemporal (ST) Validation Performances of Different Estimation Methods With the Best Estimates in Bold and the Second Best Shown in Italics

	RMSE (mm/h)			MAE (mm/h)			PBIAS			Median AE (mm/h)		
Estimation Method	T	S	ST	T	S	ST	T	S	ST	T	S	ST
CSI	3.30	3.40	3.20	2.02	1.95	1.95	−1.89	10.11	−1.51	1.19	1.03	1.12
NPR	3.60	3.50	3.53	2.40	2.26	2.35	36.98	39.44	38.01	1.55	1.40	1.52
Error variance	3.15	3.09	3.07	1.91	1.82	1.85	*−3.38*	*3.76*	*−2.20*	*1.09*	*0.96*	*1.03*
Error covariance	3.08	3.05	3.03	1.95	1.83	1.92	15.23	20.61	14.60	1.19	1.03	1.16
Error rotation	*2.97*	*3.01*	*2.92*	*1.86*	*1.79*	*1.82*	11.32	19.88	11.74	1.13	0.99	1.10
PDF overlap (Gaussian)	3.15	3.19	3.09	1.98	1.90	1.94	19.60	27.01	20.39	1.20	1.07	1.15
PDF overlap (non-Gaussian)	**2.93**	**2.93**	**2.87**	1.90	1.85	1.86	26.48	34.73	27.20	1.24	1.14	1.19
Probability aggregation	3.00	3.05	2.99	**1.84**	**1.78**	**1.81**	**5.30**	**4.18**	**−2.00**	**1.08**	**0.94**	**1.02**

Table 3. Temporal, Spatial, and Spatiotemporal Validation MAE (mm/h) of Different Estimation Methods With Respect to Rainfall Rate Thresholds, i.e., Low: < 2 mm/h, Medium: 2∼5 mm/h, and High: 5∼20 mm/h[a]

	Low			Medium			High		
Estimation Method	Temporal	Spatial	Spatiotemporal	Temporal	Spatial	Spatiotemporal	Temporal	Spatial	Spatiotemporal
CSI	0.96	0.95	0.93	1.46	1.48	1.44	3.70	3.85	3.75
NPR	1.42	1.29	1.41	1.90	1.77	1.86	4.07	4.24	4.18
Error variance	**0.76**	**0.74**	*0.74*	*1.26*	**1.26**	*1.25*	3.86	3.98	3.93
Error covariance	0.99	0.93	0.95	1.42	1.36	1.41	3.56	3.65	3.70
Error rotation	0.94	0.91	0.91	1.33	1.31	1.30	3.41	3.55	3.54
PDF overlap (Gaussian)	1.01	0.99	1.00	1.46	1.42	1.44	3.57	3.72	3.68
PDF overlap (non-Gaussian)	1.14	1.12	1.11	1.34	1.34	1.31	**3.31**	**3.44**	**3.43**
Probability Aggregation	*0.84*	**0.74**	**0.73**	**1.20**	**1.26**	**1.23**	3.61	3.86	3.80

[a]Values in bold represent the best result in each category with the second best shown in italics.

weight to large errors, as the errors are squared before they are averaged. In contrast, the MAE is a linear score where all the individual differences are weighted equally in the average like Median AE (Median absolute error) [*Chai and Draxler*, 2014]. The non-Gaussian PDF overlap method gives higher PBIAS compared to all other methods which might have influenced the RMSE. Therefore, in density-based combination approach, the probability aggregation method provides better performance among all other methods even though the PDF overlap (non-Gaussian) method results in lower RMSE than the probability aggregation method.

The probability aggregation and error variance methods are better in terms of PBIAS where the former yields positive PBIAS and the latter yields negative PBIAS. Apart from the probability aggregation method, the error rotation method gives good result in all performance criteria. On the other hand, the Gaussian and non-Gaussian PDF overlap methods show dissimilarity in performance measures. The non-Gaussian PDF overlap method gives better combination estimates (in two performance criteria, i.e., RMSE and MAE) compared to the Gaussian-based overlap method. The results clearly indicate that among all merging methods presented, the error variance method is best for point-based merging and the probability aggregation method is best for density-based merging. It can be observed that the magnitudes of the MAE and RMSE in Table 2 are not markedly different, suggesting that the influence of large outliers (which would have resulted in greater RMSEs) is low.

We have assessed the combination method using three different validation approaches, namely temporal, spatial, and spatiotemporal, to confirm whether same results hold at the ungauged location. The performance of the different combination methods remains consistent in the four assessment criteria, namely RMSE, MAE, PBIAS, and Median AE. It should be noted that the data sets are smaller for the spatiotemporal and spatial methods compared to that of the temporal method. Therefore, the difference in assessment criteria among the validation methods are not found to be significant.

The performance of each of the estimation methods was next analyzed with respect to rainfall rate by dividing into three categories: low (less than 2 mm/h), medium (2–5 mm/h), and high (5–20 mm/h). The result presented in Table 3 shows that performance of merging approaches is dependent on rainfall rates. For low rainfall rate, the error variance method shows better performance in the MAE, while probability aggregation method and the PDF overlap (non-Gaussian) method is better in medium and high rainfall rates, respectively.

We also studied the spatial structure of PBIAS, which is presented in Figure 5. The non-Gaussian PDF overlap (Figure 5d) and error rotation method (Figure 5b) produce higher positive PBIAS while the error variance (Figure 5a) and probability aggregation (Figure 5c) methods produce smaller PBIAS. The error variance-based combination method provides smaller negative PBIAS, whereas probability aggregation provides positive PBIAS at most locations. The process of forcing a zero-correlation influences the covariance matrix in the error rotation method and results in higher positive PBIAS (Figure 5b) compared to the error variance case (Figure 5a). The negative PBIAS indicates lower rainfall rates that may underestimate river discharge and thereby flash flood peaks. The NPR method gives longer PDF tails compared to that of the CSI method. This has a significant effect on the PBIAS in the non-Gaussian PDF method, which is the highest among all other methods. Synthetic tests confirmed that if one of the PDF has a thick tailed distribution, the overlap

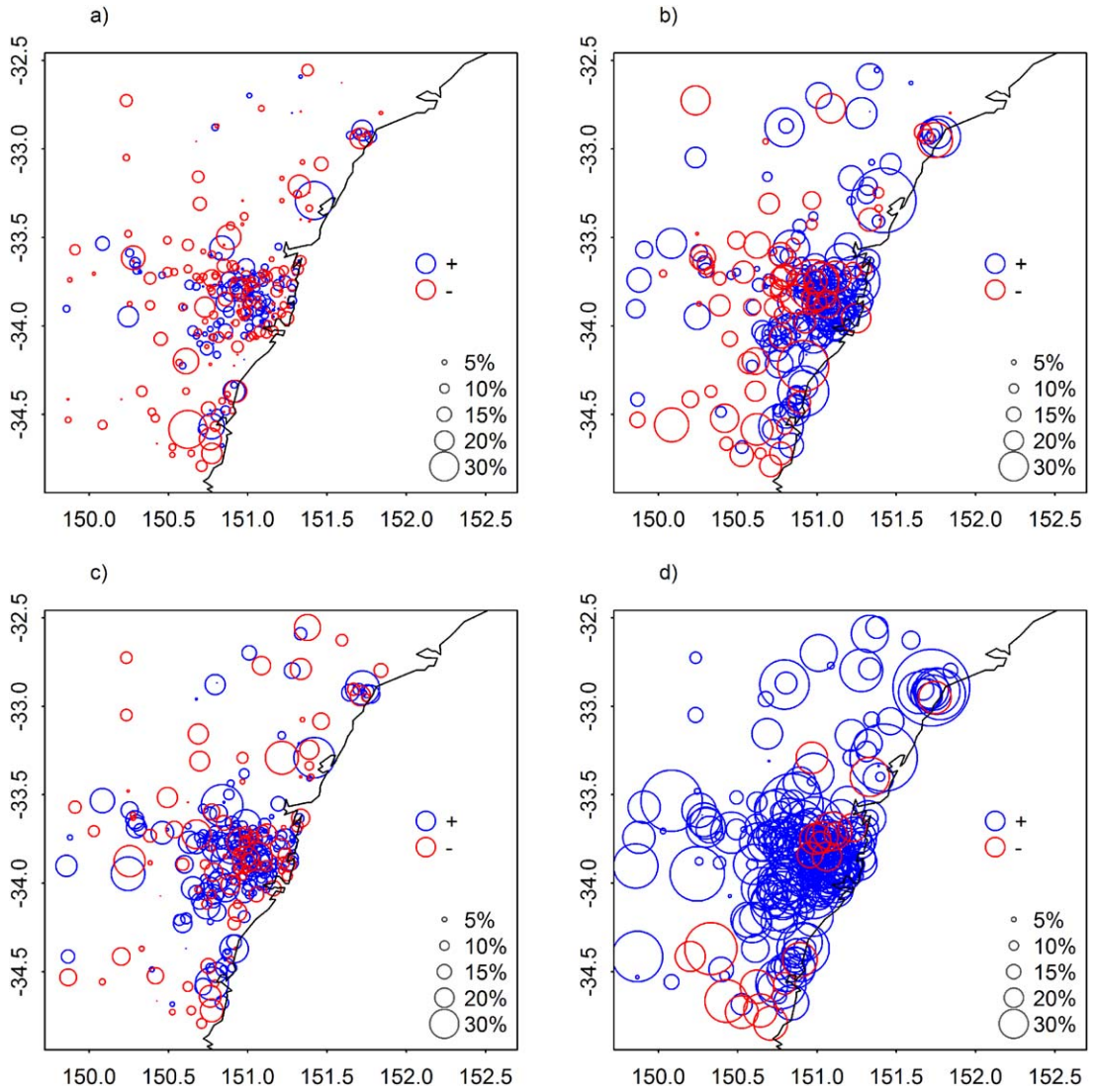

Figure 5. Percent Bias (PBIAS) of the following estimation methods: (a) error variance, (b) error rotation, (c) probability aggregation, and (d) PDF overlap (non-Gaussian). Blue circles indicate positive bias and red circles indicate negative bias.

will be very long and moments get biased toward the longer one. The PDF overlap method is designed to generate the maximum overlapping area. Therefore, the area optimization process moves toward the wider PDF and produces higher PBIAS.

To get an accurate rainfall estimates from radar-gauge merging, it is important to know the impact of rainfall magnitude on the selection of the merging method. In Figure 6, the error distribution of the different combination methods with respect to rainfall rates are presented. The gauge rainfall and the corresponding errors are presented in units of decibels (Figure 6). To illustrate the difference among the methods, we have picked three different rainfall values denoted by the symbol A, B, and C. In the error variance method, all three errors lie on the positive axis whereas, for the error rotation method they lie both in the positive and negative axis. The histogram of logerror shows that the errors are less sparse/scattered and skewness is low in probability aggregation and PDF overlap (non-Gaussian) methods. But PDF overlap (non-Gaussian) method provides smaller mean logerror compared to the probability aggregation method. RMSE in Table 2 also comply with the mean logerror. The logerror is negative in the error variance method which is associated with underestimation of rainfall. In contrast, positive logerror in the PDF overlap (non-Gaussian) method gives overestimation of rainfall. The spatial distribution of PBIAS (Figure 6) also indicates the same outcome. A logerror equal to zero implies that the estimates are unbiased.

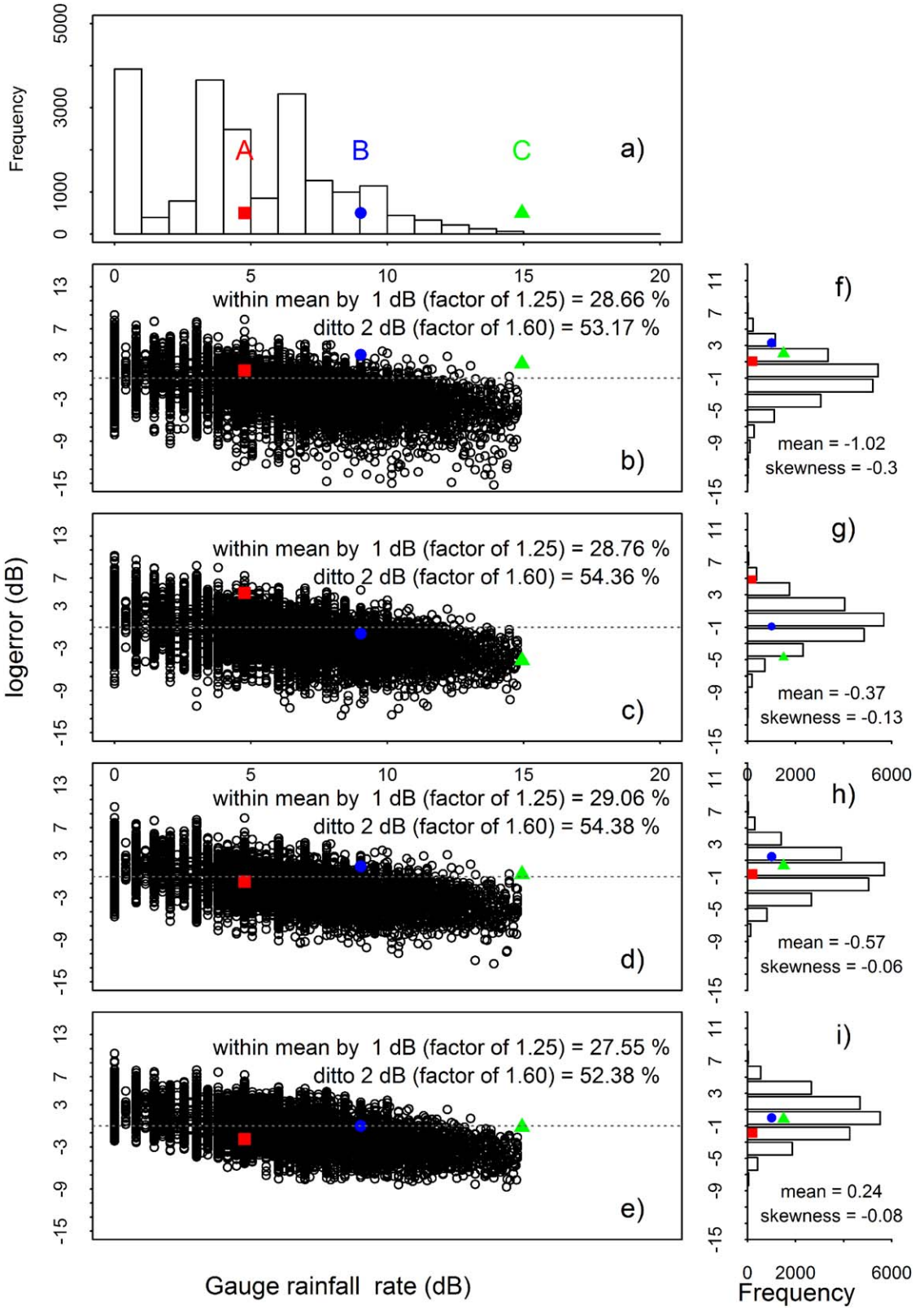

Figure 6. (a) Histogram of gauge rainfall (in decibel). The log error distribution (in decibel) of different combination methods with respect to rainfall rates: (b) error variance, (c) error rotation, (d) probability aggregation, and (e) PDF overlap (non-Gaussian). Histogram of the logerror distribution (in decibel) for different combination methods: (f) error variance, (g) error rotation, (h) Probability aggregation, and (i) PDF overlap (non-Gaussian). Three different rainfall values are denoted by the symbol A, B, and C.

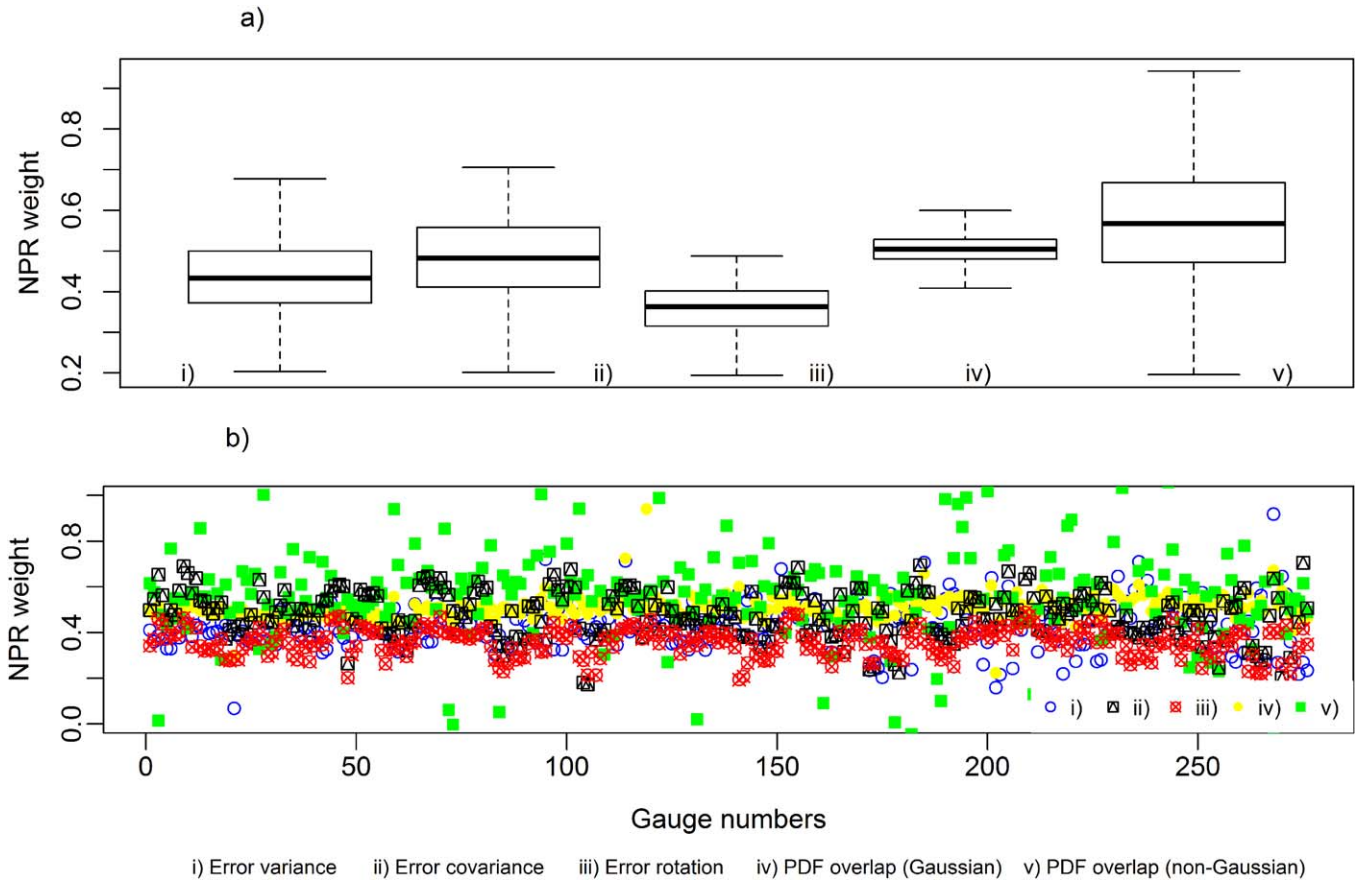

Figure 7. Variation of NPR weight for different methods for all the events (a) across all gauges and (b) across different gauges.

Results presented above show that the performance of merged estimates varies among the methods. The merged estimates depend on the weights given by CSI and NPR estimates. Therefore, we have investigated the variation of NPR weight (Figure 7) to understand the variation in merged estimates in different methods. The NPR weight in the Gaussian PDF overlap method has a narrower band whereas the non-Gaussian

Table 4. Advantages and Disadvantages of Different Merging Approach

Method	Advantages/Disadvantages	Key Attributes
Error variance	1. Simple and easy 2. Dynamic weight 3. Do not consider correlations	1. Smaller RMSE for low rainfall rate 2. Smaller negative PBIAS on spatial domain
Error covariance	1. Consider correlations 2. Dynamic weight 3. Stable estimation of the covariance matrix depends on data length	1. Gives a wider range of variability in combination weights
Error rotation	1. Consider correlations 2. Dynamic weight 3. Stable estimation of the covariance matrix depends on data length	1. Larger variability in logerror distribution 2. Higher PBIAS on spatial domain
PDF overlap (Gaussian)	1. Dynamic weight 2. Iterative weight estimation process	1. Higher RMSE 2. Higher PBIAS
PDF overlap (non-Gaussian)	1. Dynamic weight 2. Iterative weight estimation process	1. Smaller RMSE 2. Smaller MAE for high rainfall rate 3. Higher PBIAS on spatial domain
Probability aggregation	1. Static weight	1. Smaller MAE, PBIAS, Median AE 2. Smaller RMSE for medium rainfall rate 3. Smaller positive PBIAS on spatial domain

PDF overlap method shows a wider range of variability. Table 2 shows that prior to merging, PBIAS for NPR method is around 37% and for CSI method it is 2%. Therefore, the allocation of high weight to the NPR method resulted higher PBIAS in non-Gaussian PDF overlap. The NPR weight in the Gaussian PDF overlap method is around 0.50 (Figure 7), and therefore, this method does not differentiate between radar and gauge rainfall. The error covariance method gives higher combination weights with a wider range of variability to the NPR method compared to the error variance and error rotation methods. Although the NPR weight in the error rotation method is similar to that of the error variance method, the later shows more variability. It is important to note that estimation errors are uncorrelated for error variance, correlated for error covariance, and decorrelated, for the error rotation method. Therefore, the correlated errors give a wider range of variability compared to uncorrelated and decorrelated case. These observations have been summarized in the Table 4 below.

5. Discussion and Conclusion

In this paper, we have compared several radar and gauge rainfall-merging approaches. The performance of these methods has been evaluated through several attributes of interest in assessing spatial rainfall fields. Depending on the attribute of interest, different advantages and disadvantages can be noted for each of the merging methods evaluated. We emphasize that the conclusions drawn from the above results are based on the use of a fairly long data set in a validation setting. Hence, we would expect the features of the above methods to be replicated in similar applications elsewhere.

The main conclusions we draw from the results presented above are:

1. PDF overlap-based methods versus non-PDF overlap methods: while the PDF overlap methods are elegant and follow our intuitive expectation of the method to trust, they are difficult to implement and can result in fitting or sampling uncertainty especially when data is limited. The overlap methods result in the highest PBIAS across all the approaches considered, while attaining the best "fit" in terms of RMSE. Significant advantages are observed especially for high rainfall. The improved RMSE obtained with these methods may be due to the better fit in the upper tails of the distribution.
2. Nondynamic (static) versus dynamic merging methods: the only nondynamic method considered in our study is the probability aggregation method, which has one of the better performances across all the methods considered. The downside of this method is the complexity in its implementation, with the need to estimate weights as exponents using an optimization approach. Furthermore, there is an intuitive disadvantage here as this method is suboptimal using calibration data simply because the weights do not vary with time. However, given the superior performance in MAE, PBIAS, and Median AE of the method, we feel there is merit in investigating alterations that use the product weighting approach while allowing the weights to vary with time or the estimated rainfall.
3. Covariance versus noncovariance-based methods: the covariance-based methods assessed in our study have a clear advantage over the noncovariance-based approaches. This is not a new finding and has been reported by others in different contexts [*Khan et al*., 2014; *Timmermann*, 2006]. However, the PBIAS estimated is lower for the simpler noncovariance-based approach. It should be mentioned that the order of the performance across the various methods was found to remain the same when the calibration and the validation data sets were inter-changed. Hence, while the above conclusion may be a result of sampling uncertainty, it is more likely to be an outcome of the simplicity of the method being adopted.
4. Covariance versus rotation-based approach: an interesting outcome of our study was the clear advantage of the rotation-based approach over the one that used the covariance matrix alone. It should be noted that both methods require the use of the error covariances, while a further correction is involved in the rotation method. Clear improvements in all statistical attributes were visible in the error rotation method, as were improvements when the assessment was done over the various rainfall thresholds.

In conclusion, each of the methods evaluated for merging gauge-based observations with radar-derived rainfall have their own advantages and disadvantages. The error variance method is computationally inexpensive, straightforward and simple to implement. Calculation errors are much less likely to be made in the implementation of the error variance method compared to all other methods as is based on a simple mathematical calculation. In contrast, the error covariance and error rotation method use more complex algorithms, while resulting in better results. The choice of which merging method to use is a function of the

stability with which the parameters of the approach can be estimated. We recommend the use of the more complex covariance-based approaches (including the rotation method) when sufficient number of events and gauge observations are available. When this is not the case, the simpler alternatives (error variance and probability aggregation) should be adopted.

Acknowledgments
The authors gratefully acknowledge Sydney Water and the Australian Bureau of Meteorology for providing rain gauge and radar data for this study. Radar data that have been used in this study can be obtained from the Australian Bureau of Meteorology by placing a request using the Climate Data Services web page (http://www.bom.gov.au/climate/data-services/data-requests.shtml). Rain gauge data that have been used in this paper can be obtained by contacting Sydney Water (http://sydneywater.custhelp.com/app/ask). The authors acknowledge the Australian Research Council for partial funding for this work.

References

Ajami, N. K., Q. Duan, X. Gao, and S. Sorooshian (2006), Multimodel combination techniques for analysis of hydrological simulations: Application to distributed model intercomparison project results, *J. Hydrometeorol.*, *7*(4), 755–768.
Allard, D., A. Comunian, and P. Renard (2012), Probability aggregation methods in geoscience, *Math. Geosci.*, *44*(5), 545–581.
Bárdossy, A. (2006), Copula-based geostatistical models for groundwater quality parameters, *Water Resour. Res.*, *42*, W11416, doi:10.1029/2005WR004754.
Bárdossy, A., and J. Li (2008), Geostatistical interpolation using copulas, *Water Resour. Res.*, *44*, W07412, doi:10.1029/2007WR006115.
Bates, J. M., and C. W. Granger (1969), The combination of forecasts, *Oper. Res. Soc.*, *20*(4), 451–468.
Berndt, C., E. Rabiei, and U. Haberlandt (2014), Geostatistical merging of rain gauge and radar data for high temporal resolutions and various station density scenarios, *J. Hydrol.*, *508*, 88–101.
Borga, M., F. Tonelli, R. J. Moore, and H. Andrieu (2002), Long-term assessment of bias adjustment in radar rainfall estimation, *Water Resour. Res.*, *38*(11), 1226, doi:10.1029/2001WR000555.
Chai, T., and R. R. Draxler (2014), Root mean square error (RMSE) or mean absolute error (MAE)?—Arguments against avoiding RMSE in the literature, *Geosci. Model Dev.*, *7*(3), 1247–1250.
Chowdhury, S., and A. Sharma (2009), Long-range niño-3.4 predictions using pairwise dynamic combinations of multiple models, *J. Clim.*, *22*(3), 793–805.
Chowdhury, S., and A. Sharma (2010), Global sea surface temperature forecasts using a pairwise dynamic combination approach, *J. Clim.*, *24*(7), 1869–1877.
Chumchean, S., A. Seed, and A. Sharma (2004), Application of scaling in radar reflectivity for correcting range-dependent bias in climatological radar rainfall estimates, *J. Atmos. Oceanic Technol.*, *21*(10), 1545–1556.
Chumchean, S., A. Seed, and A. Sharma (2006a), Correcting of real-time radar rainfall bias using a Kalman filtering approach, *J. Hydrol.*, *317*(1-2), 123–137.
Chumchean, S., A. Sharma, and A. Seed (2006b), An integrated approach to error correction for real-time radar-rainfall estimation, *J. Atmos. Oceanic Technol.*, *23*(1), 67–79.
Clemen, R. T. (1989), Combining forecasts: A review and annotated bibliography, *Int. J. Forecast.*, *5*(4), 559–583.
Clemen, R. T., and R. L. Winkler (2007), Aggregating probability distributions, in *Advances in Decision Analysis: From Foundations to Applications*, edited by W. Edwards, R. F. Miles, and D. von Winterfeldt, pp. 154–176, Cambridge Univ. Press, Cambridge, U. K.
Creutin, J. D., G. Delrieu, and T. Lebel (1988), Rain measurement by raingage-radar combination: A geostatistical approach, *J. Atmos. Oceanic Technol.*, *5*(1), 102–115.
Delrieu, G., A. Wijbrans, B. Boudevillain, D. Faure, L. Bonnifait, and P. Kirstetter (2014), Geostatistical radar–raingauge merging: A novel method for the quantification of rain estimation accuracy, *Adv. Water Resour.*, *71*, 110–124.
Durante, F., and C. Sempi (2010), *Copula Theory and Its Applications*, edited by P. Jaworski et al., pp. 3–31, Springer, Berlin.
Ehret, U., J. Götzinger, A. Bárdossy, and G. G. S. Pegram (2008), Radar-based flood forecasting in small catchments, exemplified by the Goldersbach catchment, Germany, *Int. J. River Basin Manage.*, *6*(4), 323–329.
Fortuna, J., and D. Capson (2004), Improved support vector classification using PCA and ICA feature space modification, *Pattern Recognition*, *37*(6), 1117–1129.
Genre, V., G. Kenny, A. Meyler, and A. Timmermann (2013), Combining expert forecasts: Can anything beat the simple average?, *Int. J. Forecast.*, *29*(1), 108–121.
Georgakakos, K. P., D. J. Seo, H. Gupta, J. Schaake, and M. B. Butts (2004), Towards the characterization of streamflow simulation uncertainty through multimodel ensembles, *J. Hydrol.*, *298*(1–4), 222–241.
Gneiting, T., and R. Ranjan (2013), Combining predictive distributions (online), *J. Stat.*, *7*, 1747–1782.
Goovaerts, P. (2000), Geostatistical approaches for incorporating elevation into the spatial interpolation of rainfall, *J. Hydrol.*, *228*(1–2), 113–129.
Goudenhoofdt, E., and L. Delobbe (2009), Evaluation of radar-gauge merging methods for quantitative precipitation estimates, *Hydrol. Earth Syst. Sci.*, *13*(2), 195–203.
Haberlandt, U. (2007), Geostatistical interpolation of hourly precipitation from rain gauges and radar for a large-scale extreme rainfall event, *J. Hydrol.*, *332*(1–2), 144–157.
Hall, S. G., and J. Mitchell (2007), Combining density forecasts, *Int. J. Forecast.*, *23*(1), 1–13.
Hasan, M. M., A. Sharma, F. Johnson, G. Mariethoz, and A. Seed (2014), Correcting bias in radar Z–R relationships due to uncertainty in point rain gauge networks, *J. Hydrol.*, *519*, 1668–1676.
Hasan, M. M., A. Sharma, G. Mariethoz, F. Johnson, and A. Seed (2016), Improving radar rainfall estimation by merging point rainfall measurements within a model combination framework, *Adv. Water Resour.*, *97*, 205–218, doi:10.1016/j.advwatres.2016.09.011.
Jewell, S. A., and N. Gaussiat (2015), An assessment of kriging-based rain-gauge–radar merging techniques, Q. *J. R. Meteorol. Soc.*, *141*(691), 2300–2313.
Jones, M. C. (1993), Simple boundary correction for kernel density estimation, *Stat. Comput.*, *3*(3), 135–146.
Karunamuni, R. J., and T. Alberts (2005a), A generalized reflection method of boundary correction in kernel density estimation, *Can. J. Stat.*, *33*(4), 497–509.
Karunamuni, R. J., and T. Alberts (2005b), On boundary correction in kernel density estimation, *Stat. Methodol.*, *2*(3), 191–212.
Kazianka, H. (2013), Approximate copula-based estimation and prediction of discrete spatial data, *Stochastic Environ. Res. Risk Assess.*, *27*(8), 2015–2026.
Khan, M. Z. K., R. Mehrotra, A. Sharma, and A. Sankarasubramanian (2014), Global sea surface temperature forecasts using an improved multimodel approach, *J. Clim.*, *27*(10), 3505–3515.
Krajewski, W. F., and J. A. Smith (2002), Radar hydrology: Rainfall estimation, *Adv. Water Resour.*, *25*(8-12), 1387–1394.
Krishnamurti, T. N., C. M. Kishtawal, T. E. LaRow, D. R. Bachiochi, Z. Zhang, C. E. Williford, S. Gadgil, and S. Surendran (1999), Improved weather and seasonal climate forecasts from multimodel superensemble, *Science*, *285*(5433), 1548–1550.

Krishnamurti, T. N., C. M. Kishtawal, Z. Zhang, T. E. LaRow, D. R. Bachiochi, E. Williford, S. Gadgil, and S. Surendran (2000), Multimodel ensemble forecasts for weather and seasonal climate, *J. Clim.*, *13*(23), 4196–4216.

Liu, X., A. Ghorpade, Y. L. Tu, and W. J. Zhang (2012), A novel approach to probability distribution aggregation, *Inf. Sci.*, *188*, 269–275.

Mandapaka, P. V., W. F. Krajewski, G. J. Ciach, G. Villarini, and J. A. Smith (2009), Estimation of radar-rainfall error spatial correlation, *Adv. Water Resour.*, *32*(7), 1020–1030.

Mandapaka, P. V., G. Villarini, B. C. Seo, and W. F. Krajewski (2010), Effect of radar-rainfall uncertainties on the spatial characterization of rainfall events, *J. Geophys. Res.*, *115*, D17110, doi:10.1029/2009JD013366.

Mariethoz, G., P. Renard, and R. Froidevaux (2009), Integrating collocated auxiliary parameters in geostatistical simulations using joint probability distributions and probability aggregation, *Water Resour. Res.*, *45*, W08421, doi:10.1029/2008WR007408.

Qian, D., and J. E. Fowler (2007), Hyperspectral image compression using JPEG2000 and principal component analysis, *IEEE Geosci. Remote Sens. Lett.*, *4*(2), 201–205.

Ranjan, R. (2009), *Combining and Evaluating Probabilistic Forecasts*, Univ. of Wash., Seattle.

Ranjan, R., and T. Gneiting (2010), Combining probability forecasts, *J. R. Stat. Soc., Ser. B*, *72*(1), 71–91.

Robertson, A. W., U. Lall, S. E. Zebiak, and L. Goddard (2004), Improved combination of multiple atmospheric GCM ensembles for seasonal prediction, *Mon. Weather Rev.*, *132*(12), 2732–2744.

Seo, D.-J., and J. P. Breidenbach (2002), Real-time correction of spatially nonuniform bias in radar rainfall data using rain gauge measurements, *J. Hydrometeorol.*, *3*(2), 93–111.

Shamseldin, A. Y., and K. M. O'Connor (1999), A real-time combination method for the outputs of different rainfall-runoff models, *Hydrol. Sci. J.*, *44*(6), 895–912.

Sharma, A., D. G. Tarboton, and U. Lall (1997), Streamflow simulation: A nonparametric approach, *Water Resour. Res.*, *33*(2), 291–308.

Shih-Hau, F., L. Tsung-Nan, and L. Pochiang (2008), Location fingerprinting in a decorrelated space, *IEEE Trans. Knowledge Data Eng.*, *20*(5), 685–691.

Sideris, I. V., M. Gabella, R. Erdin, and U. Germann (2014), Real-time radar-rain-gauge merging using spatio-temporal co-kriging with external drift in the alpine terrain of Switzerland, *Q. J. R. Meteorol. Soc.*, *140*(680), 1097–1111.

Silverman, B. W. (1986), *Density Estimation for Statistics and Data Analysis*, Chapman and Hall, London, N. Y.

Sinclair, S., and G. Pegram (2005), Combining radar and rain gauge rainfall estimates using conditional merging, *Atmos. Sci. Lett.*, *6*(1), 19–22.

Smith, J., and K. F. Wallis (2009), A simple explanation of the forecast combination puzzle, *Oxford Bull. Econ. Stat.*, *71*(3), 331–355.

Smith, J. A., and W. F. Krajewski (1991), Estimation of the mean field bias of radar rainfall estimates, *J. Appl. Meteorol.*, *30*(4), 397–412.

Smith, J. A., M. L. Baeck, K. L. Meierdiercks, A. J. Miller, and W. F. Krajewski (2007), Radar rainfall estimation for flash flood forecasting in small urban watersheds, *Adv. Water Resour.*, *30*(10), 2087–2097.

Stock, J. H., and M. W. Watson (2002), Forecasting using principal components from a large number of predictors, *J. Am. Stat. Assoc.*, *97*(460), 1167–1179.

Stock, J. H., and M. W. Watson (2004), Combination forecasts of output growth in a seven-country data set, *J. Forecast.*, *23*(6), 405–430.

Tarantola, A. (2005), Inverse problem theory and methods for model parameter estimation, SIAM: Society for Industrial and Applied Mathematics.

Timmermann, A. (2006), *Handbook of Economic Forecasting*, edited by G. Elliott and A. Timmermann, pp. 135–196, Elsevier, North Holland.

Velasco-Forero, C. A., D. Sempere-Torres, E. F. Cassiraga, and J. Jaime Gómez-Hernández (2009), A non-parametric automatic blending methodology to estimate rainfall fields from rain gauge and radar data, *Adv. Water Resour.*, *32*(7), 986–1002.

Villarini, G., P. V. Mandapaka, W. F. Krajewski, and R. J. Moore (2008), Rainfall and sampling uncertainties: A rain gauge perspective, *J. Geophys. Res.*, *113*, D11102, doi:10.1029/2007JD009214.

Wasko, C., A. Sharma, and P. Rasmussen (2013), Improved spatial prediction: A combinatorial approach, *Water Resour. Res.*, *49*, 3927–3935, doi:10.1002/wrcr.20290.

Woldemeskel, F. M., B. Sivakumar, and A. Sharma (2013), Merging gauge and satellite rainfall with specification of associated uncertainty across Australia, *J. Hydrol.*, *499*, 167–176.

Zhang, Y., and J. A. Smith (2003), Space-time variability of rainfall and extreme flood response in the Menomonee River basin, Wisconsin, *J. Hydrometeorol.*, *4*(3), 506–517.